THE JOURNAL OF PHYSICAL CHEMISTRY C

Article

Cite This: J. Phys. Chem. C 2017, 121, 23788-23792

pubs.acs.org/JPCC

Ice Nucleation in Periodic Arrays of Spherical Nanocages

Simone Mascotto,[†] Wolfhard Janke,[‡] and Rustem Valiullin*[,¶]

[†]Institute of Inorganic and Applied Chemistry, University of Hamburg, 20146 Hamburg, Germany

[‡]Institute of Theoretical Physics, University of Leipzig, 04103 Leipzig, Germany

[¶]Felix Bloch Institute for Solid State Physics, University of Leipzig, 04103 Leipzig, Germany

Supporting Information

ABSTRACT: A silicious material containing massive array of spherical nanocages connected to each other by small micropores was used to study ice nucleation in confined water under conditions of well-defined pore geometry. By purposefully selecting small size of the interconnecting pores below 2 nm, ice nucleation and growth were limited to occur only within the nanocages. By exploitation of nuclear magnetic resonance, ice nucleation rates at different temperatures were accurately measured. These rates were obtained to be substantially higher than those typically observed for micrometer-sized water droplets in air. In addition, the occurrence of correlations between ice nucleation in one nanocage with the phase state in the adjacent cages were observed. These results have important implication for a deeper understanding of ice nucleation, especially in confined geometries.

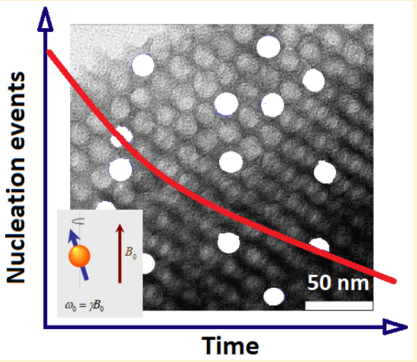

INTRODUCTION

Predicting ice nucleation rates is a cornerstone problem of statistical thermodynamics with broad implications for many branches of natural and life sciences.[1−3] Despite long history of experimental and theoretical studies, many aspects of this phenomenon still remain a matter of intense research.[4−12] Experimental exploration of ice nucleation in bulk liquids is a challenging task, in particular due to interference between nucleation and crystal growth. A useful strategy to overcome this problem is to prepare small water droplets, e.g., in the form of an aerosol, and to follow their crystallization frequencies at different supercoolings.[13−18] In this approach, a particular care needs to be paid to take account of an unavoidable distribution of the droplet sizes. Alternatively, water imbibed into porous materials can be used as a route to decrease the liquid volume sizes. By using porous solids with ordered porosities,[19−21] crystallization of water in well-defined pore geometries can be studied. Porous materials with both disordered and ordered pore systems have already been used for establishing the phase diagrams for confined water, i.e., for determining the freezing/melting temperatures as a function of the pore size.[22−28] At the same time, investigations of the crystallization kinetics in confined geometries, which may contribute to better understanding of the ice nucleation phenomena, are scarcely reported.

In this work we exploit a siliceous porous solid FDU-12 containing a periodic array of spherical cages with 12 nm pore diameter, which are interconnected via small pores with the pore sizes below 2 nm, to study homogeneous ice nucleation. Because the pore space in the material used is globally interconnected, some bulk-like properties of water, e.g., the possibility of long-range density fluctuations or of pressure equilibration via mass transfer, become preserved. On the other hand, due to a purposeful choice of the pore size below 2 nm, in which the ice formation is strongly suppressed,[29,30] macroscopic crystal growth triggered by homogeneous ice nucleation in the spherical cages turns out to be excluded. Hence, this system provides a remarkable option to probe ice nucleation in macroscopic samples with the crystal growth mode being intentionally suppressed. Notably, cavitation of gas bubbles was successfully probed using this strategy.[31]

EXPERIMENTAL SECTION

The FDU-12 material used in this work was synthesized according to the procedure described by Morishige with an hydrothermal treatment step at 80 °C for 1 day.[32] The porosity and morphology of the material were comprehensively characterized using nitrogen physisorption, small-angle X-rays scattering (SAXS) and electron microscopy (TEM) (see Supporting Information). The silica possesses a pore structure composed of spherical cages with the diameter d of 12 nm arranged in a face-centered cubic lattice with the lattice constant of about 25 nm. These cages are connected via pores with the pore sizes below 2 nm. By using the cooperative self-assembly procedure the final material resulted in macroscopically extended particles of several micrometers with inner ordered pore structure. Prior to the measurements, the samples were outgassed using a turbo-molecular vacuum pump and thereafter saturated with purified water under vacuum atmosphere in order to prevent the formation of air bubbles.

Received: August 25, 2017
Revised: October 3, 2017
Published: October 3, 2017

DOI: 10.1021/acs.jpcc.7b08490
J. Phys. Chem. C 2017, 121, 23788−23792

In one sample, the amount of water was such that only the mesopore space was filled with water, and any excess water between the FDU-12 particles was excluded; in another sample, excess water was provided.

To probe the crystallization process we used NMR relaxometry allowing to distinguish between frozen and liquid water and thus to probe the phase change dynamics. Because of a substantial difference in the nuclear magnetic transverse relaxation rates in intrapore water (several tens of milliseconds) and in crystalline ice (tens of microseconds),[33] the NMR signals of the two phases can easily be separated. This is done by applying an NMR relaxation filter composed of a pair of 90° and 180° radio frequency excitation pulses (Hahn echo pulse sequence) separated by the time interval τ of hundreds of microseconds.[34] In this way, the NMR spin−echo signal measured is contributed by only nuclear spins (water protons) of the water molecules which are found in the liquid phase. The Hahn spin−echo signal intensities measured in our experiments are reported here as normalized functions, S, and reflect thus the relative fraction of nonfrozen water in the samples. In what follows, S, measured as a function of temperature, will be referred to as "freezing curve".

Temperature calibration in the sample was performed using a Pt100 sensor. In order to determine the water diffusivity at low temperatures, the pulsed field gradient technique of NMR has been used.[35] In this method, the Hahn echo pulse sequence was complemented by the pulses of the magnetic field gradients allowing for spatial encoding and decoding of the nuclear spin positions and thus measuring their mean square displacements (see Supporting Information).

RESULTS AND DISCUSSION

Some typical freezing curves are shown in parts a and b of Figure 1. To obtain them, the samples were first slowly cooled down to T_i = 240 K. At this temperature no freezing was observed; i.e., the signal measured remained constant over time. Freezing was initiated by quickly quenching temperature from T_i to a desired one T, at which the freezing kinetics were measured. Parts a and b of Figure 1 reveal that, besides an expected enhancement of the ice nucleation rates with decreasing T, the freezing rates are found to decrease with increasing evolution time after the temperature quenches.

The well-defined pore structure of the FDU-12 material used allows for a reasonable interpretation of the experimentally measured freezing kinetics. It is well established experimentally that upon cooling water confined in cylindrical pores with the pore sizes below about 2.9 nm no crystalline ice is formed down to 180 K.[29,36] Hence, at T > 180 K, the crystalline ice phase can be formed *only* in the spherical cages, but not in the micropores. Once an ice seed is nucleated in a cage, it grows to fill the entire cage with the ice crystal. The time scale of this growth process is many orders of magnitude shorter than the experimental times of our experiments. Notably, a one-to-two monolayer thick liquid-like water film adjacent to the pore walls remains in a high mobility, liquid-like state ensuring minimization of the total free energy.[33,37] Because ice formed in a cage cannot aid the ice formation in the neighboring ones, the freezing kinetics measured in our experiments reflect the sole process of homogeneous ice nucleation in the individual cages. This is in contrast to interconnected pore systems in which crystal growth may be dominant.[38] In what follows we analyze how the nucleation rates can be derived from the experimental data and what they depend on.

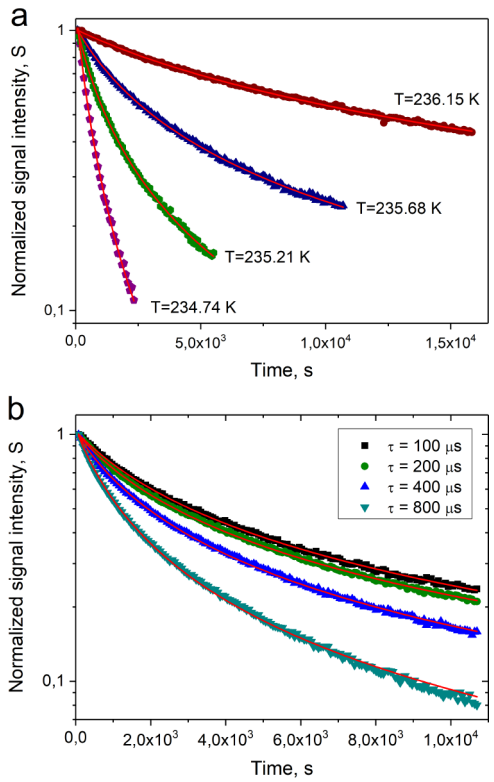

Figure 1. Freezing kinetics, i.e., normalized Hahn spin−echo signal intensities S obtained (a) with the interpulse delay τ = 100 μs and at different temperatures T and (b) with different τ at T = 235.68 K. The solid lines show the best fits of eq 2 to the experimental data.

Quite generally, one may consider two possible scenarios for freezing in our samples. Namely, it may proceed either (i) homogeneously over the material, i.e., the ice nucleation events in different cages are spatially uncorrelated, or (ii) in a spatially correlated way, giving rise to propagating nucleation fronts.[39] These scenarios, however, are not supported by the experimental evidence. If the nucleation events would occur randomly across the material, then it is straightforward to show that the freezing kinetics should be of an exponential form, $S \propto \exp(-R_0 t)$, with R_0 being the genuine nucleation rate in one cage. The experimentally obtained kinetics in parts a and b of Figure 1 exhibit, however, a strongly nonexponential form.

The second scenario contradicts the observation that the freezing kinetics are found to depend on the relaxation delay time τ in the NMR pulse-sequence (see Figure 1b). This dependency results from water diffusion between different pools of mobile water in the material under study. The transverse nuclear magnetic relaxation rates of water phase in the cages filled completely with water and in the liquid-like layers in the cages containing ice in their core parts are notably different. In the latter case the relaxation rates are substantially higher. Hence, with increasing τ, i.e., with increasing length of the diffusion pathways of the water molecules, the chance to encounter an ice-containing cage, where the nuclear magnetization relaxes more rapidly, is higher. During the time intervals τ from hundred microseconds to several milliseconds used in our experiments, water molecules displace by the distances $\sqrt{2D\tau}$, where D is the water diffusivity in the sample, shorter than 150 nm. This estimate is based on the independently measured diffusion coefficients $D \approx 5 \times 10^{-12}$ m^2/s (see Supporting Information) using the pulsed field gradient

DOI: 10.1021/acs.jpcc.7b08490
J. Phys. Chem. C 2017, 121, 23788−23792

technique of NMR.[35] If the nanocages containing only liquid water and nanocages containing ice would form separated regions with macroscopic extensions, the τ-dependency could not be observed due to a relatively low interfacial area between these regions and hence negligible molecular exchange between them. That means that the two types of the cages should be well intermixed on the length scale of 150 nm.

A compromise scenario, in which the experimental observations can reasonably be explained, is the occurrence of the locally correlated nucleation events. Here it is assumed that the nucleation probabilities in the nanocages are correlated with the phase state in the nearest-neighbor cages. The governing equation for such process is

$$\frac{dN}{dt} = R(N_0 - N)\left(1 - \frac{N}{N_0}\right)^n \quad (1)$$

where N_0 is the total number of cages, N is the number of cages containing ice, and R is the nucleation rate. The last term $(1 - N/N_0)^n$ in the product on the right-hand side of eq 1 describes, in a mean-field-like manner, the nearest-neighbor correlations. Degree of these correlations is modeled using a (positive) exponent n, which, in what follows, will be referred to as 'coupling constant'. Thus, $n = 0$ means that the nucleation events and phase state in the nearest-neighbor cages are completely uncorrelated, while $n > 0$ implies that the presence of the ice-containing cages lowers the nucleation probability. Note that $1 - N/N_0$, which is the relative fraction of the water-containing cages, is equal to the normalized signal intensity S measured in the experiments. Hence, the following functional form for S is readily obtained:

$$S = (1 + nRt)^{-1/n} \quad (2)$$

Equation 2 nicely reproduces the experimentally measured kinetics for all temperatures studied and the results of the best fit for both R and n are shown in parts a and b of Figure 2. In what follows, we first discuss the nucleation rates of Figure 2a and then the coupling phenomenon resulting in $n > 0$ as seen in Figure 2b.

As it has been noted earlier, R is found to be a function of τ (see Figure 2a) caused by water diffusion. To obtain accurately the genuine nucleation rate per cage, $R_0 = R(\tau \to 0)$, a simple phenomenological model relating the measured rates to the genuine ones has been developed (see Supporting Information). The model predicts that

$$R(\tau) = R_0\left(1 + A\frac{\sqrt{2D\tau}}{r}\right)^3 \quad (3)$$

where r is the nanocage radius and A is a proportionality constant determining which part of the nuclear magnetization in the volume $(\sqrt{2D\tau})^3$ is lost due to the occurrence of an ice-containing cage in the center of this volume. For the purpose of this work, we fitted eq 3 to the data of Figure 2a to obtain R_0. The latter are shown in Figure 3.

The rates obtained experimentally in this work for water confined to nanocages formed in a siliceous material are found to be a few orders of magnitude higher than those typically measured in the experiments in this temperature range by using micrometer-sized water droplets in air.[8,11,40,41] Moreover, the temperature dependency of R_0 deviates from the pattern $\ln(R) \propto T$ often seen in the experiments in this temperature range.

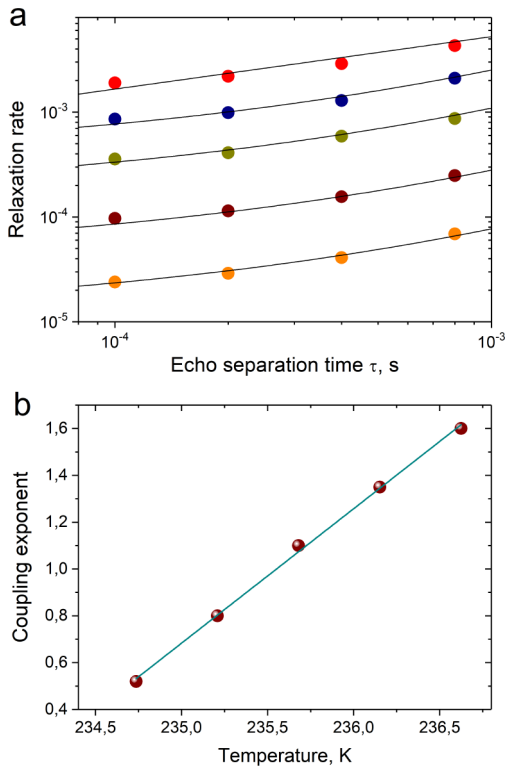

Figure 2. (a) Freezing rates R and (b) coupling constants n obtained by fitting eq 2 to the experimental data on the freezing kinetics obtained with different τ and at different T. The coupling constants n were allowed to vary while fitting the experimental data obtained with τ = 100 μs. This value obtained was then fixed while fitting the data obtained with longer τ.

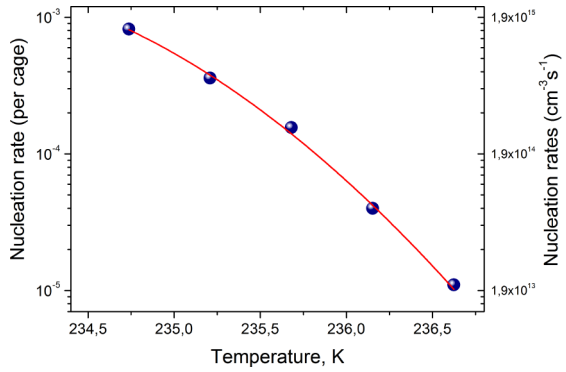

Figure 3. Intrinsic nucleation rates R_0 obtained by fitting eq 3 to the experimental data on the apparent kinetic rates obtained for different τ shown in Figure 2a. The solid line shows the best fit with T_H = 233.57 K and α = 1.88 (see also Supporting Information).

We find that the data of Figure 3 are accurately captured by an empirical equation

$$R_0 = C\ \exp\{-B(T - T_H)^\alpha\} \quad (4)$$

in which a power-law divergence of the energy barriers upon approaching the temperature $T_H \approx 233.6$ K, the temperature of spontaneous ice nucleation, is assumed.[42]

Quite generally, one may associate these observations either with a notable decrease of the water volume as compared to other experimental studies or with the presence of the solid walls. With respect to the former one, it has been anticipated in the literature that, due to a substantial increase of the water

DOI: 10.1021/acs.jpcc.7b08490
J. Phys. Chem. C 2017, 121, 23788−23792

droplet surface-to-volume ratio, the (possible) occurrence of surface-assisted nucleation[10,16,43−45] may dominate over bulk nucleation. A satisfactory experimental confirmation of this phenomenon is, however, lacking. Molecular simulations, on the other hand, deliver controversial conclusions, which depend strongly on the molecular models used for water. Thus, the Laplace pressure was anticipated to strongly suppress the nucleation rates in the nanosized mW water droplets,[17] while the use of TIP4P/ice force field was shown, in contrast, to enhance the nucleation rates in thin water films by several orders of magnitude.[46] In the simulations mentioned only free water interfaces were addressed. In our case, however, confined water was in contact with the silica surface, which is wet by water. Whether surface-assisted nucleation is effective under these conditions is difficult to answer.

On considering further solid surface-assisted mechanisms, which may lead to an enhancement of the nucleation rates, the occurrence of heterogeneous nucleation seems to be improbable due to a mismatch between the silica surface and ice crystalline structures. At the same time, it is worth noting that the spherical cages in the FDU-12 material are not closed and have openings formed by the small pores in the silica walls. This gives rise to particular geometries of the pore space close to the openings, which may feature wedge-like motifs. In line with a recent work by Bi et al.,[47] one may anticipate that these geometric patterns may favor the formation of metastable topological defects and thus lead the enhanced nucleation rates. Experimental prove of this scenario may be possible by a purposeful variation of the geometric features of the interconnecting pores and this will be a focus of our subsequent studies. Alternatively, because no excess liquid between FDU-12 particles was present, strong surface interaction could result in negative pressures[48] and, hence, alter the nucleation process. In order to verify whether this phenomenon can be responsible for the high nucleation rates observed, we have performed additional experiments with excess water surrounding the FDU-12 particles. The results obtained were qualitatively similar (see Supporting Information), only the relaxation rates were found to be slightly lower thus rendering the negative pressure effects questionable.

In contrast, the observed slowing down of the crystallization rates with progressing crystallization, as indicated by $n > 0$ in Figure 3, may be anticipated to at least partly be caused by increasing pressure. Indeed, the formation of ice in the cages leads to expelling of water out of the FDU-12 particles. The liquid at the particle boundary freezes immediately. If the excess water is supplied intentionally it is already found in the frozen state at the temperatures at which the experiments are performed. Thus, the FDU-12 particles may become surrounded by an ice shell giving rise to pressure increase upon progressive crystallization. Whether the pressure increase alone can lead to the functional form of eq 2, i.e., whether the term $(1 - N/N_0)^n$ in this equation arises due to the pressure effect, shall be addressed in future studies.

CONCLUSIONS

In summary, we present the first experimental study of ice nucleation kinetics in water confined in an ordered mesoporous silica material. Two important results obtained are (i) an accurate determination of the nucleation rates, which turn out to be several orders of magnitude higher than those typically measured in micrometer-sized water droplets in air and (ii) observation of the slowing down of the nucleation rates with progressive crystallization. These two observations pose an interesting open questions both for theory and experiment. A fine-tunability of the pore structure in the material studied allows to efficiently address how the cage size, size of the connecting pores, and surface chemistry affect the nucleation process and this will be in the focus of our future work.

ASSOCIATED CONTENT

Supporting Information

The Supporting Information is available free of charge on the ACS Publications website at DOI: 10.1021/acs.jpcc.7b08490.

Material structure characterization, water diffusivities in FDU-12, additional experimental results on nucleation rates (PDF)

AUTHOR INFORMATION

Corresponding Author

*(R.V.) E-mail: valiullin@uni-leipzig.de. Telephone: +49 341 9732515.

ORCID

Rustem Valiullin: 0000-0001-5028-7642

Notes

The authors declare no competing financial interest.

ACKNOWLEDGMENTS

The work is supported by the German Science Foundation (DFG, Project VA 463/6-1). The authors thank Nail Fatkullin (Kazan) and Michael Fröba (Hamburg) for valuable discussions.

REFERENCES

(1) Koop, T.; Luo, B. P.; Tsias, A.; Peter, T. Water activity as the determinant for homogeneous ice nucleation in aqueous solutions. *Nature* **2000**, *406*, 611−614.

(2) Auer, S.; Frenkel, D. Prediction of absolute crystal-nucleation rate in hard-sphere colloids. *Nature* **2001**, *409*, 1020−1023.

(3) Ehre, D.; Lavert, E.; Lahav, M.; Lubomirsky, I. Water freezes differently on positively and negatively charged surfaces of pyroelectric materials. *Science* **2010**, *327*, 672−675.

(4) Matsumoto, M.; Saito, S.; Ohmine, I. Molecular dynamics simulation of the ice nucleation and growth process leading to water freezing. *Nature* **2002**, *416*, 409−413.

(5) Mallamace, F.; Broccio, M.; Corsaro, C.; Faraone, A.; Majolino, D.; Venuti, V.; Liu, L.; Mou, C. Y.; Chen, S. H. Evidence of the existence of the low-density liquid phase in supercooled, confined water. *Proc. Natl. Acad. Sci. U. S. A.* **2007**, *104*, 424−428.

(6) Moore, E. B.; Molinero, V. Structural transformation in supercooled water controls the crystallization rate of ice. *Nature* **2011**, *479*, 506−509.

(7) Li, K. Y.; Xu, S.; Shi, W. X.; He, M.; Li, H. L.; Li, S. Z.; Zhou, X.; Wang, J. J.; Song, Y. L. Investigating the effects of solid surfaces on ice nucleation. *Langmuir* **2012**, *28*, 10749−10754.

(8) Manka, A.; Pathak, H.; Tanimura, S.; Wolk, J.; Strey, R.; Wyslouzil, B. E. Freezing water in no-man's land. *Phys. Chem. Chem. Phys.* **2012**, *14*, 4505−4516.

(9) Russo, J.; Romano, F.; Tanaka, H. New metastable form of ice and its role in the homogeneous crystallization of water. *Nat. Mater.* **2014**, *13*, 733−739.

(10) Espinosa, J. R.; Sanz, E.; Valeriani, C.; Vega, C. Homogeneous ice nucleation evaluated for several water models. *J. Chem. Phys.* **2014**, *141*, 18C529.

(11) Ickes, L.; Welti, A.; Hoose, C.; Lohmann, U. Classical nucleation theory of homogeneous freezing of water: thermodynamic and kinetic parameters. *Phys. Chem. Chem. Phys.* **2015**, *17*, 5514−5537.

DOI: 10.1021/acs.jpcc.7b08490
J. Phys. Chem. C 2017, 121, 23788−23792

(12) Amann-Winkel, K.; Bohmer, R.; Fujara, F.; Gainaru, C.; Geil, B.; Loerting, T. Colloquium: Water's controversial glass transitions. *Rev. Mod. Phys.* **2016**, *88*, 20.
(13) Turnbull, D. Kinetics of solidification of supercooled liquid mercury droplets. *J. Chem. Phys.* **1952**, *20*, 411−424.
(14) Wood, G. R.; Walton, A. G. Homogeneous nucleation kinetics of ice from water. *J. Appl. Phys.* **1970**, *41*, 3027−3036.
(15) Huang, J. F.; Bartell, L. S. Kinetics of homogeneous nucleation in the freezing of large water clusters. *J. Phys. Chem.* **1995**, *99*, 3924−3931.
(16) Atkinson, J. D.; Murray, B. J.; O'Sullivan, D. Rate of homogenous nucleation of ice in supercooled water. *J. Phys. Chem. A* **2016**, *120*, 6513−6520.
(17) Li, T.; Donadio, D.; Galli, G. Ice nucleation at the nanoscale probes no mans land of water. *Nat. Commun.* **2013**, *4*, 1887.
(18) Espinosa, J. R.; Zaragoza, A.; Rosales-Pelaez, P.; Navarro, C.; Valeriani, C.; Vega, C.; Sanz, E. Interfacial free energy as the key to the pressure-induced deceleration of ice nucleation. *Phys. Rev. Lett.* **2016**, *117*, 135702.
(19) Ciesla, U.; Schüth, F. Ordered mesoporous materials. *Microporous Mesoporous Mater.* **1999**, *27*, 131−149.
(20) Morell, J.; Gungerich, M.; Wolter, G.; Jiao, J.; Hunger, M.; Klar, P. J.; Fröba, M. Synthesis and characterization of highly ordered bifunctional aromatic periodic mesoporous organosilicas with different pore sizes. *J. Mater. Chem.* **2006**, *16*, 2809−2818.
(21) Li, W.; Yue, Q.; Deng, Y. H.; Zhao, D. Y. Ordered mesoporous materials based on interfacial assembly and engineering. *Adv. Mater.* **2013**, *25*, 5129−5152.
(22) Baker, J. M.; Dore, J. C.; Behrens, P. Nucleation of ice in confined geometry. *J. Phys. Chem. B* **1997**, *101*, 6226−6229.
(23) Morishige, K.; Yasunaga, H.; Uematsu, H. Stability of cubic ice in mesopores. *J. Phys. Chem. C* **2009**, *113*, 3056−3061.
(24) Petrov, O.; Furó, I. A study of freezing-melting hysteresis of water in different porous materials. Part II: surfactant-templated silicas. *Phys. Chem. Chem. Phys.* **2011**, *13*, 16358−16365.
(25) Miyatou, T.; Ohashi, R.; Ida, T.; Kittaka, S.; Mizuno, M. An NMR study on the mechanisms of freezing and melting of water confined in spherically mesoporous silicas SBA-16. *Phys. Chem. Chem. Phys.* **2016**, *18*, 18555−18562.
(26) Jiang, Q.; Ward, M. D. Crystallization under nanoscale confinement. *Chem. Soc. Rev.* **2014**, *43*, 2066−2079.
(27) Suzuki, Y.; Steinhart, M.; Butt, H. J.; Floudas, G. Kinetics of ice nucleation confined in nanoporous alumina. *J. Phys. Chem. B* **2015**, *119*, 11960−11966.
(28) Yao, Y.; Ruckdeschel, P.; Graf, R.; Butt, H. J.; Retsch, M.; Floudas, G. Homogeneous nucleation of ice confined in hollow silica spheres. *J. Phys. Chem. B* **2017**, *121*, 306−313.
(29) Morishige, K.; Kawano, K. Freezing and melting of water in a single cylindrical pore: The pore-size dependence of freezing and melting behavior. *J. Chem. Phys.* **1999**, *110*, 4867−4872.
(30) Kittaka, S.; Takahara, S.; Matsumoto, H.; Wada, Y.; Satoh, T. J.; Yamaguchi, T. Low temperature phase properties of water confined in mesoporous silica MCM-41: Thermodynamic and neutron scattering study. *J. Chem. Phys.* **2013**, *138*, 204714−9.
(31) Rasmussen, C. J.; Vishnyakov, A.; Thommes, M.; Smarsly, B. M.; Kleitz, F.; Neimark, A. V. Cavitation in metastable liquid nitrogen confined to nanoscale pores. *Langmuir* **2010**, *26*, 10147−10157.
(32) Morishige, K.; Yoshida, K. Neck Size of ordered cage-type mesoporous silica FDU-12 and origin of gradual desorption. *J. Phys. Chem. C* **2010**, *114*, 7095−7101.
(33) Valiullin, R.; Furó, I. The morphology of coexisting liquid and frozen phases in porous materials as revealed by exchange of nuclear spin magnetization followed by H-1 nuclear magnetic resonance. *J. Chem. Phys.* **2002**, *117*, 2307−2316.
(34) Petrov, O. V.; Furó, I. NMR cryoporometry: Principles, applications and potential. *Prog. Nucl. Magn. Reson. Spectrosc.* **2009**, *54*, 97−122.
(35) Valiullin, R. *Diffusion NMR of Confined Systems: Fluid Transport in Porous Solids and Heterogeneous Materials*; The Royal Society of Chemistry: Cambridge, U.K., 2017.
(36) Alabarse, F. G.; Haines, J.; Cambon, O.; Levelut, C.; Bourgogne, D.; Haidoux, A.; Granier, D.; Coasne, B. Freezing of water confined at the nanoscale. *Phys. Rev. Lett.* **2012**, *109*, 035701.
(37) Dash, J. G.; Rempel, A. W.; Wettlaufer, J. S. The physics of premelted ice and its geophysical consequences. *Rev. Mod. Phys.* **2006**, *78*, 695−741.
(38) Dvoyashkin, M.; Khokhlov, A.; Valiullin, R.; Kärger, J. Freezing of fluids in disordered mesopores. *J. Chem. Phys.* **2008**, *129*, 154702−6.
(39) Vincent, O.; Sessoms, D. A.; Huber, E. J.; Guioth, J.; Stroock, A. D. Drying by cavitation and poroelastic relaxations in porous media with macroscopic pores connected by nanoscale throats. *Phys. Rev. Lett.* **2014**, *113*, 134501.
(40) Murray, B. J.; Broadley, S. L.; Wilson, T. W.; Bull, S. J.; Wills, R. H.; Christenson, H. K.; Murray, E. J. Kinetics of the homogeneous freezing of water. *Phys. Chem. Chem. Phys.* **2010**, *12*, 10380−10387.
(41) Riechers, B.; Wittbracht, F.; Hutten, A.; Koop, T. The homogeneous ice nucleation rate of water droplets produced in a microfluidic device and the role of temperature uncertainty. *Phys. Chem. Chem. Phys.* **2013**, *15*, 5873−5887.
(42) Binder, K. Nucleation barriers, spinodals, and the Ginzburg criterion. *Phys. Rev. A: At., Mol., Opt. Phys.* **1984**, *29*, 341−349.
(43) Djikaev, Y. S. Effect of the surface-stimulated mode on the kinetics of homogeneous crystal nucleation in droplets. *J. Phys. Chem. A* **2008**, *112*, 6592−6600.
(44) Kuhn, T.; Earle, M. E.; Khalizov, A. F.; Sloan, J. J. Size dependence of volume and surface nucleation rates for homogeneous freezing of supercooled water droplets. *Atmos. Chem. Phys.* **2011**, *11*, 2853−2861.
(45) Scholz, J.; Etter, M.; Haas, D.; Meyer, A.; Kornowski, A.; Sazama, U.; Mascotto, S. Pore geometry effect on the synthesis of silica supported perovskite oxides. *J. Colloid Interface Sci.* **2017**, *504*, 346−355.
(46) Haji-Akbari, A.; Debenedetti, P. G. Computational investigation of surface freezing in a molecular model of water. *Proc. Natl. Acad. Sci. U. S. A.* **2017**, *114*, 3316−3321.
(47) Bi, Y.; Cao, B.; Li, T. Enhanced heterogeneous ice nucleation by special surface geometry. *Nat. Commun.* **2017**, *8*, 15372.
(48) Soper, A. K. Radical re-appraisal of water structure in hydrophilic confinement. *Chem. Phys. Lett.* **2013**, *590*, 1−15.

DOI: 10.1021/acs.jpcc.7b08490
J. Phys. Chem. C 2017, 121, 23788−23792